Triple approach to determination of the c-axis penetration depth in BSCCO crystals

M. R. Trunin, Yu. A. Nefyodov, D. V. Shovkun, and A. A. Zhukov,

Institute of Solid State Physics, 142432, Chernogolovka, Moscow district, Russia

N. Bontemps

Laboratoire de Physique du Solide ESPCI, 10 rue Vauquelin, 75231 Paris cedex 05, France

A. Buzdin and M. Daumens

Laboratoire de Physique Théorique, Université Bordeaux I, 33405 Talence Cedex, France

H. Enriquez

SRSIM/DRECAM/DSM, CEA-Saclay, 91191 Gif sur Yvette cedex, France

T. Tamegai

Department of Applied Physics, The University of Tokyo, Hongo, Bunkyo-ku, 113-8656, Japan

The c-axis penetration depth λ_c in $Bi_2Sr_2CaCu_2O_{8+\delta}$ (BSCCO) single crystals as a function of temperature has been determined using three high-frequency techniques, namely: (i) measurements of the ac-susceptibility at a frequency of 100 kHz for different sample alignments with respect to the ac magnetic field; (ii) measurements of the surface impedance in both superconducting and normal states of BSCCO crystals at 9.4 GHz; (iii) measurements of the surface barrier field $H_J(T) \propto 1/\lambda_c(T)$ at which Josephson vortices penetrate into the sample. Careful analysis of these measurements, including both numerical solution of the electrodynamic problem of the magnetic field distribution in an anisotropic plate at an arbitrary temperature and influence of defects in the sample, has allowed us to estimate $\lambda_c(0) \approx 50$ μm in BSCCO crystals overdoped with oxygen ($T_c \approx 84$ K) and $\lambda_c(0) \approx 150$ μm at the optimal doping level ($T_c \approx 90$ K). The results obtained by different techniques are in reasonable agreement.

KEY WORDS: High-frequency response; anisotropy; penetration depth; BSCCO crystals; surface barrier; defects.

I. INTRODUCTION

Study of anisotropy of the magnetic field penetration depth as a function of temperature in high-T_c superconductors (HTS) advance considerably our understanding of pairing mechanism in these materials. It is known (see, e.g., Ref.[1] and references therein) that in-plane penetration depth $\Delta\lambda_{ab}(T) \propto T$ in the range $T < T_c/3$ in high-quality HTS samples at the optimal level of doping, and this observation can be interpreted the most simply in the d-wave model of the high-frequency response of HTS. Measurements of out-of-plane or c-axis penetration depth $\lambda_c(T)$ are quoted less frequently than those of $\lambda_{ab}(T)$. Most of such data published so far were derived from microwave measurements of the surface impedance of HTS crystals[2–10]. There is no consensus about $\Delta\lambda_c(T)$ at low temperatures. Even in high-quality YBCO crystals, which are the most studied objects, one can find both linear, $\Delta\lambda_c(T) \propto T^{3,8}$, and quadratic dependences[10] in the range $T < T_c/3$. In BSCCO materials, the shape of $\Delta\lambda_c(T)$ depends on the level of oxygen doping: in samples with maximal $T_c \simeq 90$ K $\Delta\lambda_c(T) \propto T$ at low temperatures[6,7]; at higher oxygen contents (overdoped samples) T_c is lower and the linear function $\Delta\lambda_c(T)$ transforms to a quadratic one[7]. The common feature of all microwave experiments is that the change in the ratio

$\Delta\lambda_c(T)/\lambda_c(0)$ is smaller than in $\Delta\lambda_{ab}(T)/\lambda_{ab}(0)$ because in all HTS $\lambda_c(0) \gg \lambda_{ab}(0)$. Another possibility to determine c-axis penetration depth is the measurements of the first penetration field of Josephson vortices. In quasi-2D systems, their penetration may be impeded by a surface barrier, the value of which is inversely proportional to $\lambda_c(T)$[11]. The quantitative estimates of $\lambda_c(T)$ deduced from the surface barrier data were however disputed[12]. Furthermore, $\lambda_c(T)$ is also inversely proportional to the plasma frequency[13,14] which is usually assigned to Josephson plasma resonance frequency modified by the field-dependent interlayer phase coherence[13,15]. However, this interpretation is still controversial[16]. Therefore, independent measurements of $\lambda_c(T)$ are of interest. To date, all the above mentioned properties have been studied separately. It is the aim of this paper to apply together three different techniques to the determination of the absolute value of $\lambda_c(T)$ in order to obtain unambiguous results: (i) ac-susceptibility measurements of BSCCO crystals have allowed us to determine the temperature variation $\Delta\lambda_c(T)$; ii) cavity perturbation technique and electrodynamic analysis of the surface impedance anisotropy is used to determine both the variations and absolute values of $\lambda_c(T)$ and $\lambda_{ab}(T)$; (iii) the first penetration field of Josephson vortices is measured and shown to be related to $\lambda_c(T)$.

II. ELECTRODYNAMIC BASIS OF THE MEASUREMENTS

The electrodynamics of layered anisotropic HTS is characterized by the components σ_{ab} and σ_c of the conductivity tensor. In the normal state, ac field penetrates in the direction of the c-axis through the skin depth $\delta_{ab} = \sqrt{2/\omega\mu_0\sigma_{ab}}$ and in the CuO_2 plane through $\delta_c = \sqrt{2/\omega\mu_0\sigma_c}$. In the superconducting state all parameters δ_{ab}, δ_c, $\sigma_{ab} = \sigma'_{ab} - i\sigma''_{ab}$, and $\sigma_c = \sigma'_c - i\sigma''_c$ are complex. In the temperature range $T < T_c$, if $\sigma' \ll \sigma''$, the field penetration depths are given by the formulas $\lambda_{ab} = \sqrt{1/\omega\mu_0\sigma''_{ab}}$, $\lambda_c = \sqrt{1/\omega\mu_0\sigma''_c}$. In the close neighborhood of T_c, if $\sigma' > \sigma''$, the decay of magnetic field in the superconductor is characterized by the functions $\mathrm{Re}\,(\delta_{ab})$ and $\mathrm{Re}\,(\delta_c)$, which turn to δ_{ab} and δ_c at $T \geq T_c$, respectively.

In this paper we present the results of high-frequency measurements of anisotropy of two BSCCO single crystals with various levels of oxygen doping. The first sample (#1), characterized by a lower critical temperature, $T_c \approx 84$ K (slightly overdoped), has dimensions $a \times b \times c \simeq 0.8 \times 1.8 \times 0.03$ mm^3. The second (#2, $a \times b \times c \simeq 1.5 \times 1.5 \times 0.1$ mm^3) is almost optimally doped ($T_c \approx 90$ K).
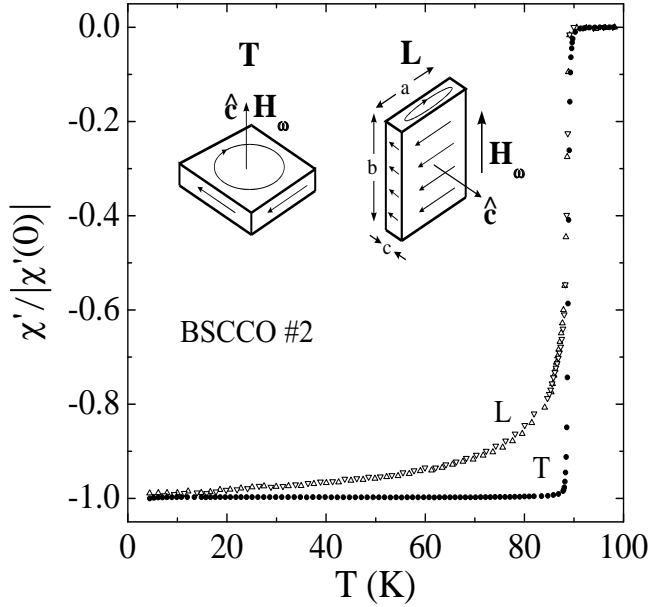

FIG. 1. Curves of the ac-susceptibility of sample #2 versus temperature in different orientation with respect to ac magnetic field: $\mathbf{H}_\omega \parallel \mathbf{c}$ (full circles); $\mathbf{H}_\omega \perp \mathbf{c}$, $\mathbf{H}_\omega$ is parallel to the b-edge of the crystal (up triangles); $\mathbf{H}_\omega \perp \mathbf{c}$, $\mathbf{H}_\omega$ is parallel to the a-edge of the crystal (down triangles). Left-hand inset: transverse (T) orientation, $\mathbf{H}_\omega \parallel \mathbf{c}$, the arrows on the surfaces show directions of the screening current. Right-hand inset: Longitudinal (L) orientation, $\mathbf{H}_\omega \perp \mathbf{c}$.

For determination of both $\lambda_{ab}(T)$ and $\lambda_c(T)$ components of the penetration depth we measured the temperature dependences of the Q-factor and the frequency shift δf of the resonant circuit for different sample alignments with respect to the ac magnetic field $\mathbf{H}_\omega$: in the transverse (T) orientation, $\mathbf{H}_\omega \parallel \mathbf{c}$, when the screening current flows in the ab-plane of the crystal and in the longitudinal (L) orientation, $\mathbf{H}_\omega \perp \mathbf{c}$, with currents running in the directions of both CuO_2 planes and the c-axis (insets to Fig. 1). In the first case the values of Q(T) and $\delta f(T)$ are directly connected with in-plane penetration depth $\lambda_{ab}(T)$ at $T < T_c$ and skin depth $\delta_{ab}(T)$ at $T \geq T_c$[1]. Both lengths are smaller than the thickness of the crystal. In the second L-orientation at $T < 0.9\,T_c$ the penetration depth is still smaller than characteristic sample dimensions. But at $T > 0.9\,T_c$ the lengths λ_c and δ_c are comparable to the width of the crystal. In order to analyze our measurements in both superconducting and normal states, we used formulae for field distributions in an anisotropic long strip ($b \gg a, c$) in the L-orientation. These formulae neglect the effect of ac-faces of the crystal, if $\mathbf{H}_\omega$ is parallel to the b-edge of the crystal (inset on the right of Fig. 1), but take into account the size effect. At an arbitrary temperature, the measured quantities are expressed in terms of the complex parameter μ introduced in Ref.[17], which is controlled by the components $\sigma_{ab}(T)$ and $\sigma_c(T)$ of the conductivity tensor through the penetration depths δ_{ab} and δ_c[18]:

$$\mu = \frac{8}{\pi^2}\sum_n \frac{1}{n^2}\left\{\frac{\tan(\alpha_n)}{\alpha_n} + \frac{\tan(\beta_n)}{\beta_n}\right\},$$

$$\alpha_n^2 = -\frac{a^2}{\delta_c^2}\left(\frac{i}{2} + \frac{\pi^2}{4}\frac{\delta_{ab}^2}{c^2}n^2\right), \quad \beta_n^2 = -\frac{c^2}{\delta_{ab}^2}\left(\frac{i}{2} + \frac{\pi^2}{4}\frac{\delta_c^2}{a^2}n^2\right), \quad (1)$$

where the sum is performed over odd integers $n > 0$. In the superconducting state, if $\sigma' \ll \sigma''$, the parameter μ is real:

$$\mu = \frac{8}{\pi^2}\sum_n \frac{1}{n^2}\left\{\frac{\tanh(\tilde{\alpha}_n)}{\tilde{\alpha}_n} + \frac{\tanh(\tilde{\beta}_n)}{\tilde{\beta}_n}\right\},$$

$$\tilde{\alpha}_n^2 = \frac{a^2}{\lambda_c^2}\left(\frac{1}{4} + \frac{\pi^2}{4}\frac{\lambda_{ab}^2}{c^2}n^2\right), \quad \tilde{\beta}_n^2 = \frac{c^2}{\lambda_{ab}^2}\left(\frac{1}{4} + \frac{\pi^2}{4}\frac{\lambda_c^2}{a^2}n^2\right). \quad (2)$$

III. AC-SUSCEPTIBILITY MEASUREMENTS

The first approach to determination of the c-axis penetration depth $\lambda_c(T)$ in BSCCO single crystals is based on measuring the ac-susceptibility $\chi = \chi' - i\chi''$ at a frequency of 100 kHz. The imaginary part χ'' of χ is proportional to the energy dissipation in the sample and the real part χ' is proportional to the shielding of magnetic field. Ac-susceptibility is characterized by the components of the conductivity tensor and, hence, allows to determine the penetration depth λ. Experimentally it is possible if the penetration depth is comparable to the sample dimension. So the ac-susceptibility measurements are usually adapted to the superconducting powders whose grain size is comparable to λ. However, since $\lambda_c(0)$ in BSCCO single crystals is relatively large, we managed to determine $\lambda_c(T)$ from the temperature dependences of $\chi'(T)$.

As an example, figure 1 shows the temperature dependences $\chi'(T)/|\chi'(0)|$ in sample #2 for three different sample alignments with respect to the ac magnetic field: in the T-orientation, $\mathbf{H}_\omega \parallel \mathbf{c}$, (full circles); in the L-orientation, $\mathbf{H}_\omega \perp \mathbf{c}$, ($\mathbf{H}_\omega$ is parallel to the b-edge of the crystal, up triangles); in the L-orientation, whose difference from the previous configuration is that the sample is turned around the c-axis through $90°$ (down triangles). Fig. 1 clearly shows that at $T < T_c$ $\chi'_{ab}(T)$ is notably smaller in the T-orientation than $\chi'_{ab+c}(T)$ in the L-orientation (the subscripts of χ' denote the direction of the screening current). The coincidence of $\chi'_{ab+c}(T)$ curves at $\mathbf{H}_\omega \perp \mathbf{c}$ and the small width of the superconducting transition at $\mathbf{H}_\omega \parallel \mathbf{c}$ ($\Delta T_c < 1$ K) indicate that the quality of the tested sample #2 is fairly high.

In the superconducting state at $T < 0.9\,T_c$ we find that $\lambda_{ab} \ll c$ and $\lambda_c \ll a$. In this case, we derive from Eq. (2) a simple relation between the real parts of μ and χ:

$$\mu' = 1 + \chi' = \frac{2\lambda_c}{a} + \frac{2\lambda_{ab}}{c}\ . \qquad (3)$$
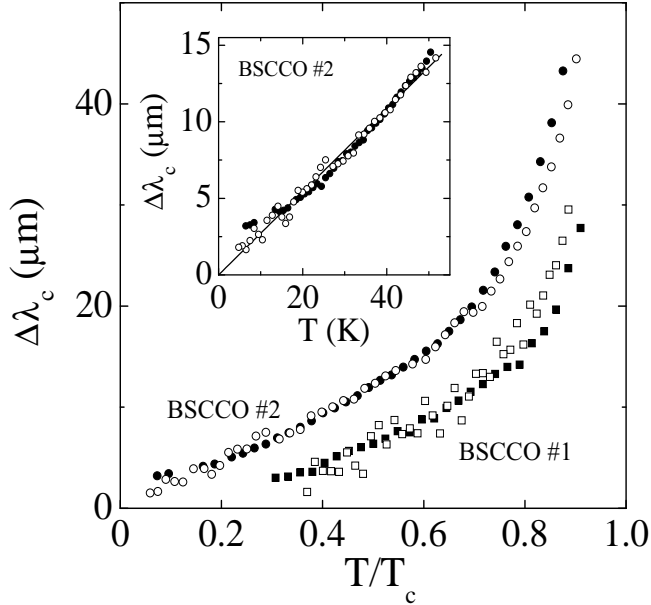

FIG. 2. Temperature dependences $\Delta\lambda_c$ in sample #1 (squares) and #2 (circles) at $T < 0.9\,T_c$. Open symbols plot low-frequency measurements, full symbols show microwave data. The inset shows low temperature sections of the $\Delta\lambda_c$ curves in sample #2.

Figure 2 shows measurements of $\Delta\lambda_c(T)$ in sample #1 (squares) and sample #2 (circles) at $T < 0.9\,T_c$. The open symbols plot low-frequency measurements obtained

from $\chi'(T)$ in accordance with Eq. (3), the full symbols plot microwave measurements (see the next section). Agreement between these measurements is fairly good, but in fitting together experimental data from sample #2 (upper curve) we had to divide by a factor of 1.8 all $\Delta\lambda_c(T)$ derived from measurements of ac-susceptibility using Eq. (3). The cause of the difference between $\Delta\lambda_c(T)$ measured in sample #2 at different frequencies is not quite clear[18].

The curves of $\Delta\lambda_c(T)$ at $T < 0.5\,T_c$ plotted in Fig. 2 are almost linear: $\Delta\lambda_c(T) \propto T$. The inset to Fig. 2 shows the low-temperature section of the curve of $\Delta\lambda_c(T)$ in sample #2. Its slope is 0.3 μm/K and equals that from Ref.[7]. Note that changes in $\Delta\lambda_c(T)$ are smaller in the oxygen-overdoped sample #1 than in sample #2.

We also estimated $\lambda_c(0)$ on the base of absolute measurements of the susceptibility $\chi'_c(0)$ and we obtained $\lambda_c(0) \approx 70$ μm for sample #1 and $\lambda_c(0) \approx 210$ μm for sample #2.

IV. CAVITY PERTURBATION TECHNIQUE

The second technique of determination $\lambda_c(T)$ is measuring the difference $\Delta(1/Q)$ (Δf) between reciprocal Q's (resonant frequency shifts) of a cavity with a sample inside and the empty cavity as functions of temperature at a frequency $f = 9.4$ GHz. These parameters are related to the surface impedance $Z_s = R_s + iX_s$ components through the geometrical factor Γ_s of the sample: $R_s = \Gamma_s\Delta(1/Q)$, $\Delta X_s = -2\Gamma_s\Delta f/f$[1]. The penetration depth is $\lambda(T) = X_s(T)/\omega\mu_0$ at $T < T_c$. In order to determine the absolute value of $X_s = -2\Gamma_s\delta f/f$, where δf is the frequency shift relative to that which would be measured for a sample with perfect screening and no penetration of the microwave fields, one needs the constant parameter $f_0 = \Delta f(T) - \delta f(T)$. In HTS this constant can be derived from microwave measurements in the normal state.

In the T-orientation f_0 can be derived from the condition that the real and imaginary parts of the impedance should be equal above T_c (normal skin-effect)[19]. Given f_0, we can calculate the conductivity $\sigma_{ab}(T) = \sigma'_{ab} - i\sigma''_{ab} = i\omega\mu_0/Z_s^2(T)$ at all T. The temperature dependences of $\sigma'_{ab}(T)$ (open squares) and $\sigma''_{ab}(T)$ (open circles) are shown in Fig. 3a and Fig. 3b for crystals #1 and #2 respectively. Note that $\sigma'_{ab}(T)$ in Fig. 3b does not have a broad peak at low temperatures, typical for $\sigma'_{ab}(T)$ in high-quality HTS. The reason for that is the rather large value of the residual surface resistance: $R_{\mathrm{res}} \equiv R_s(T \to 0) \approx 0.5$ mΩ in the ab-plane of the sample #2[20], R_{res} was four times less in the sample #1.
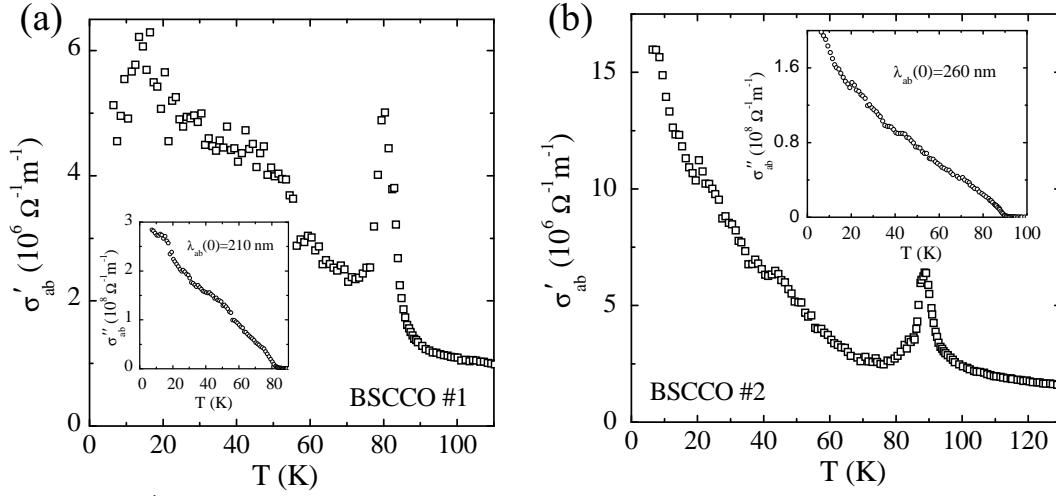
FIG. 3. Conductivities $\sigma'_{ab}(T)$ (open squares) of two BSCCO single crystals #1 (fig. a) and #2 (fig. b) at 9.4 GHz, extracted from the surface impedance measurements. The insets show $\sigma''_{ab}(T) = \lambda^2_{ab}(0)/\lambda^2_{ab}(T)$ data (open circles).

In the L-orientation of a crystal shaped as a long strip the quantities $\Delta(1/Q)$ and δf are expressed in terms of the complex function $\mu = \mu' - i\mu''$ from Eq. (1) or $\chi = (-1 + \mu)$:

$$\Delta(1/Q) - 2i\,\delta f/f = i\gamma\mu v/V, \tag{4}$$

where v and $V = 58$ cm^3 are the volumes of the sample and cavity respectively, $\gamma = 10.6$ is a constant of our cavity[1]. In the superconducting state at $T < 0.9\,T_c$ the expression for μ is given by Eq. (3). The curves of $\Delta\lambda_c(T)$ in sample #1 (full squares) and sample #2 (full circles), measured by cavity perturbation technique and obtained using Eqs. (3), (4), are shown in Fig. 2.
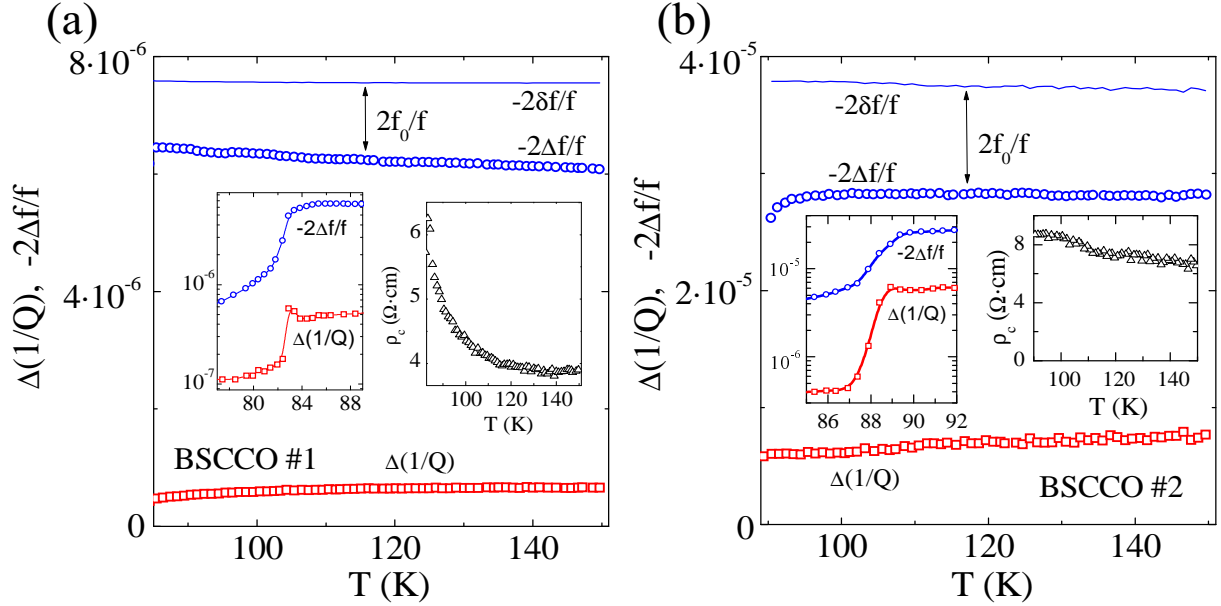

FIG. 4. Temperature dependences of $\Delta(1/Q)$ (open squares) and $-2\Delta f/f$ (open circles) at $\mathbf{H}_\omega \parallel \mathbf{b}$ of sample #1 (fig. a) and sample #2 (fig. b) at $T > T_c$. Solid lines show the functions $-2\delta f(T)/f$ deriving from Eqs. (4) and (1). Left-hand insets: $\Delta(1/Q)$ and $-2\Delta f/f$ as functions of temperature in the neighborhood of T_c. Right-hand insets: $\rho_c(T)$ (triangles).

We can estimate $\lambda_c(0)$ by comparing of $\Delta(1/Q)$ and $\Delta f = \delta f - f_0$ measurements taken in the T- and L-orientations to numerical calculations by Eqs. (1) and (4), which take account of the size effect in the high-frequency response of an anisotropic crystal. The procedure of comparison for sample #1 and #2 is illus-

trated by Fig. 4a and Fig. 4b respectively. Unlike the case of the T-orientation, the measured temperature dependence of $\Delta(1/Q)$ in the L-orientation deviates from $(-2\Delta f/f)$ owing to the size effect. Using the measurements of $\sigma_{ab}(T)$ at $T > T_c$ in the T-orientation (Fig. 3), alongside the data on $\Delta(1/Q)$ in the L-orientation (open

4

squares in Fig. 4), from Eqs. (1) and (4) we obtain the curves of $\rho_c(T) = 1/\sigma_c(T)$ shown in the right-hand insets to Fig. 4a and Fig. 4b for crystals #1 and #2. Further, using the functions $\sigma_c(T)$ and $\sigma_{ab}(T)$, we calculate $(-2\delta f/f)$ versus temperature for $T > T_c$, which are plotted by the solid lines in Fig. 4. These lines are approximately parallel to the experimental curves of $-2\Delta f/f$ in the L-orientation (open circles in Fig. 4). The difference $-2(\delta f - \Delta f)/f$ yields the additive constant f_0. Given f_0 and $\Delta f(T)$ measured in the range $T < T_c$, we also obtain $\delta f(T)$ in the superconducting state in the L-orientation. As a result, with due account of $\lambda_{ab}(T) = \sqrt{1/\omega\mu_0\sigma''_{ab}(T)}$ (insets to Fig. 3), we derive from Eqs. (4) and (3) $\lambda_c(0)$, which equals approximately $\lambda_c(0) \approx 50\ \mu$m in sample #1 and 150 μm in sample #2. These results are in reasonable agreement with our ac-susceptibility measurements if we take into consideration the fact that the accuracy of λ_c measurements is rather poor and the error can be up to 30%. The temperature dependences of $\sigma''_c(T)$ for both BSCCO single crystals are shown in Fig. 5.
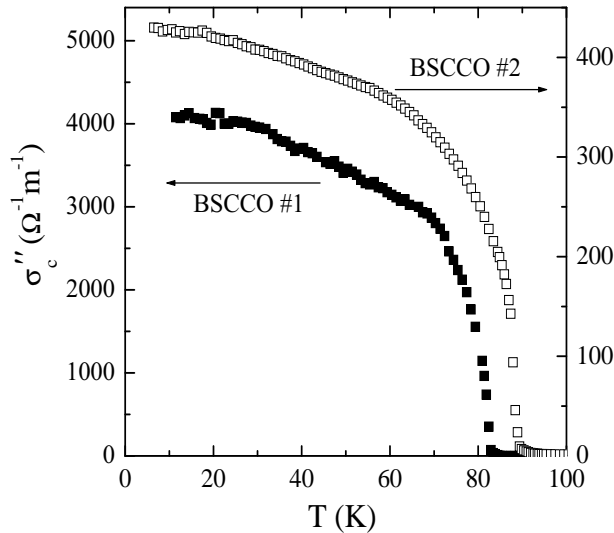

FIG. 5. Conductivities $\sigma''_c(T)$ of BSCCO single crystals #1 (left scale) and #2 (right scale) at 9.4 GHz, obtained by comparing the measurements of $\Delta(1/Q)$ and $\Delta f = \delta f - f_0$ to numerical calculations by Equation (1).

V. MICROWAVE ABSORPTION MEASUREMENTS IN A STATIC MAGNETIC FIELD: SURFACE BARRIER AND INFLUENCE OF DEFECTS

An alternative technique for the determination of $\lambda_c(0)$ is based on the measurements of the magnetic field $H_J(T)$ at which Josephson vortices penetrate into the sample.

In the experiment the microwave absorption measured in the L-orientation as a function of the static magnetic field (0-30 Oe) parallel to the CuO_2 layers exhibits a notable increase at the field $H_J(T)$[21]. Figure 6 displays the change of microwave dissipation, starting from zero field
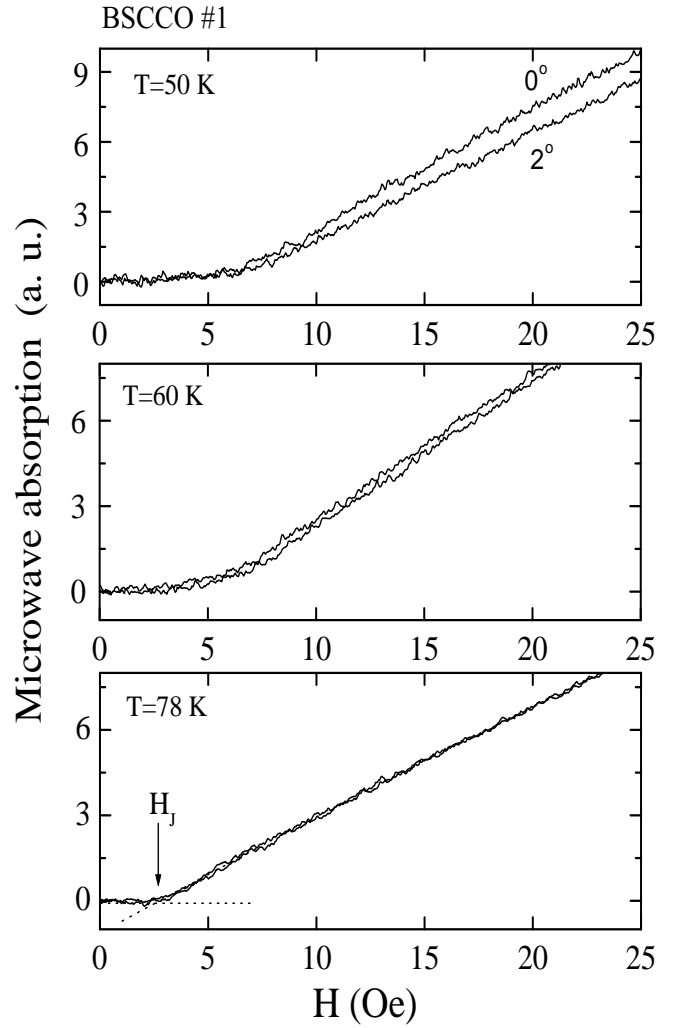

FIG. 6. Microwave absorption as a function of the applied field $\mathbf{H}$ at 3 temperatures, for 2 orientations ($0°$ and $2°$) of the $\mathbf{H}$ with respect to the ab-plane. The onset of dissipation, indicated by the arrow, occurs at the penetration field $H_J(T)$.

(within ± 0.1 Oe) measured in sample #1 for various orientations of the applied field close to the ab-plane ($0°$ and $2°$) and in a low-field range: $0 \leq H \leq 25$ Oe, at three typical temperatures ($T = 78$ K, 65 K, 50 K). After each field sweep, the sample was warmed through T_c and then cooled again in zero field, in order to avoid any possible vortex pinning when studying the penetration starting from zero field. The dissipation of Josephson vortices is characterized by the fact that it does not depend on the angle (Fig. 6), as long as these vortices remain locked. As the field increases, an onset in the dissipation occurs at a temperature-dependent field $H_J(T)$, which we associate to Josephson vortices entering the sample. As in Ref.[22], we choose to define $H_J(T)$ as the field value where the microwave absorption exceeds the experimental accuracy. The field thus determined is plotted in Fig. 7. The error bars take into account both the noise and the estimated drift of the signal with time.
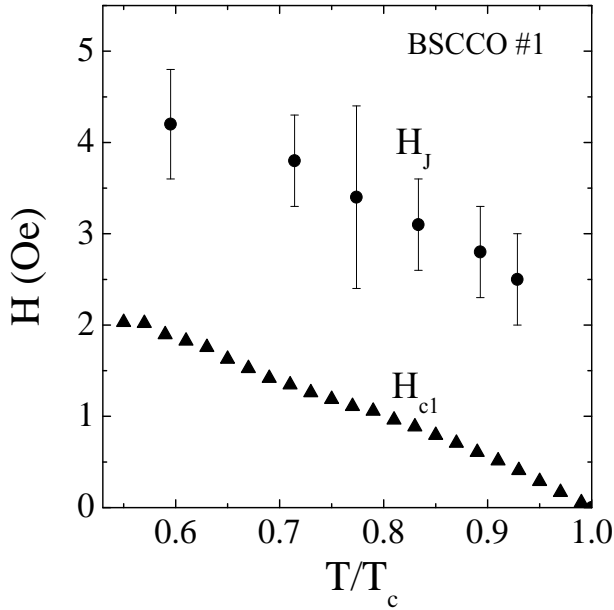
FIG. 7. Plot of $H_J(T)$ (full circles) for BSCCO crystal #1. Triangles display the upper bond of $H_{c1}(T)$ using $\lambda_{ab}(0) = 2100$ Å and $\lambda_c(0) = 10$ μm. The temperature variations $\Delta\lambda_{ab}(T)$ and $\Delta\lambda_c(T)$ are taken from the present work.

The magnitude of $H_J(T)$ is too large to be associated with the first thermodynamic critical field $H_{c1}(T)$ for Josephson vortices[23]:

$$H_{c1}(T) = \frac{\phi_0}{4\pi\lambda_{ab}(T)\lambda_c(T)}[\ln\lambda_{ab}(T)/d + 1.12], \quad (5)$$

where ϕ_0 is the flux quantum and d is the interlayer distance (~ 15 Å in BSCCO). Indeed, in Fig. 7 the triangles demonstrate an upper bound for $H_{c1}(T)$. Here, we take 2100 Å as a lower bound for $\lambda_{ab}(0)$[24,25], and 10 μm for $\lambda_c(0)$[26-30]. We use the temperature dependence for $\Delta\lambda_{ab}(T)$ from $\sigma''_{ab}(T) = 1/[\omega\mu_0\lambda_{ab}^2(T)]$ shown in the inset of Fig. 3a, and $\Delta\lambda_c(T)$ (squares in Fig. 2). It is clearly seen that neither the absolute value (too small compared to the experimental data) nor the temperature dependence (quasi-linear) agrees with the $H_J(T)$ data.

It is therefore quite natural to assume that a Bean-Livingston surface barrier[31] impedes magnetic flux penetration into the sample and yields a higher entry field $H_{SB}(T)$. This assumption is also supported by the irreversible behavior of the dissipation upon flux exit[21]. In anisotropic superconductors in the quasi-2D regime, which holds in BSCCO up to temperatures very close to T_c, the field $H_{SB}(T)$ was shown to be related only to the c-axis penetration length through[11] :

$$H_{SB}(T) = \frac{\phi_0}{4\pi\lambda_c(T)d}. \quad (6)$$

The surface barrier might thus account for the observed value of the penetration field. Also, since $H_{SB}(T)$ grows as $1/\lambda_c(T)$ (instead of $1/\lambda_{ab}\lambda_c(T)$), it is expected that the temperature dependence could show a better

agreement. So we derive from the $H_J(T)$ data an effective penetration depth $\lambda_J(T) = \phi_0/[4\pi H_J(T)d]$ on the analogy of Eq. (6). The data are shown in Fig. 8 (full squares). We then try to determine $\lambda_c(0) = \lambda_J(T) - \Delta\lambda_c(T)$ so as to fit $\lambda_J(T)$ using the measured by ac-susceptibility and cavity perturbation technique $\Delta\lambda_c(T)$ (full circles in Fig. 8 extend the lower curve in Fig. 2 to higher temperatures). We find that both sets of data, namely $\lambda_J(T)$ and $\Delta\lambda_c(T)$, cannot be reconciled for any value we may assume for $\lambda_c(0)$ in the entire temperature range. Therefore, the interpretation cannot be so simple.
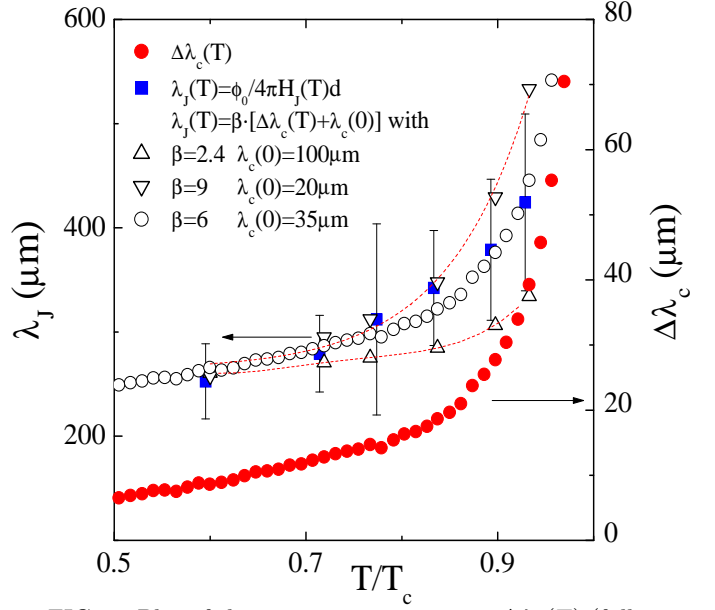

FIG. 8. Plot of the temperature variation $\Delta\lambda_c(T)$ (full circles, right scale) and of the effective length $\lambda_J(T)$ which is associated to a surface barrier for the penetration of Josephson vortices (full squares, left scale) in sample #1. Open circles display the best fit using $\lambda_c(0) = 35$ μm and a scaling factor $\beta = 6$. Open symbols show the best fits using $\lambda_c(0) = 20$ μm (down triangles) and $\lambda_c(0) = 100$ μm (up triangles).

More detailed quantitative investigation and calculations of the penetration field in the presence of edge or surface defects, have led us to the conclusion that $H_J(T)$ is eventually controlled by such surface irregularities[21].

We have carried out several checks (cleaving sample, cutting deep and wide grooves at the ab-plane, rotation crystal along it's c-axis) and established that large defects, greater or comparable with the penetration depth, within the ab-planes or at the edges of the crystal do not destroy the surface barrier (no significant change in the onset field of the microwave absorption was observed). However, if the dimensions of the surface irregularities are smaller than λ then their presence can strongly influence the screening current distribution. Indeed, the entrance field is deduced from the balance between the vortex attraction to the surface and the pushing force exerted by the screening current at the minimum distance ξ (the vortex core size)[31,32]. Near a small scratch the

6

current density can be many times larger than near the flat surface. This may substantially increase the force pushing vortices inside the superconductor and then decrease the surface barrier and the entrance field. As shown in Ref.[21], in the specific case of a thin groove with the depth $b \gtrsim d$ at the surface, the penetration field $H_J(T) = H_{SB}(T)/\beta$, where parameter $\beta = (b/d)^{1/2} > 1$. Based on this estimation, we have attempted to fit our data on

$$\lambda_J(T) = \frac{\phi_0 \beta}{4\pi H_{SB}(T)d} = \beta\left[\Delta\lambda_c(T) + \lambda_c(0)\right], \qquad (7)$$

using two adjustable parameters β and $\lambda_c(0)$ (see Fig. 8). We have obtained the best fit at $\beta = 6$ (or $b \sim 500$ Å) and $\lambda_c(0) = (35 \pm 15)$ μm in Eq. (7), which is in agreement with our measurements by the first two methods. We also show in Fig. 8 smaller and larger values for $\lambda_c(0)$. They allow us to set the uncertainty about our determination of the penetration depth. We can also fit the data in the presence of a slit at the edge of the crystal[21]. The depth of the edge slit should be of the order of 10 μm, which is still small with respect to $\lambda_c(0)$. The key result in this latter case is that it yields the same absolute value for $\lambda_c(0)$.

VI. CONCLUSION

In conclusion, we have used three high-frequency techniques in studying anisotropic properties of BSCCO single crystals. The results obtained by different techniques are in reasonable agreement. We have observed almost linear dependences $\Delta\lambda_c(T) \propto T$ at low temperatures. We have also determined the absolute value of $\lambda_c(0)$, which is a factor of three higher in the optimally doped BSCCO sample than in the overdoped crystal. The ratio between the slopes of curves of $\Delta\lambda_c(T)$ in the range $T \ll T_c$ is the same. These facts could be put down to dependences of $\lambda_c(0)$ and $\Delta\lambda_c(T)$ on the oxygen content in these samples. At the same time, the set of our experiments suggest very strongly the influence of defects in the samples, which relates the first penetration field $H_J(T)$ of Josephson vortices to the c-axis penetration depth. In order to draw ultimate conclusions concerning the nature of the transport properties along the c-axis in BSCCO single crystals, studies of more samples with various oxygen contents are needed.

VII. ACKNOWLEDGEMENTS

[1] M. R. Trunin, *Physics–Uspekhi* **41**, 843 (1998); *J. Superconductivity* **11**, 381 (1998).

[2] T. Shibauchi, H. Kitano, K. Uchinokura, A. Maeda, T. Kimura, and K. Kishio, *Phys. Rev. Lett.* **72**, 2263 (1994).

[3] J. Mao, D. H. Wu, J. L. Peng, R. L. Greene, and S. M. Anlage, *Phys. Rev. B* **51**, 3316 (1995).

[4] H. Kitano, T. Shibauchi, K. Uchinokura, A. Maeda, H. Asaoka, and H. Takei, *Phys. Rev. B* **51**, 1401 (1995).

[5] D. A. Bonn, S. Kamal, K. Zhang, R. Liang, and W. N. Hardy, *J. Phys. Chem. Solids* **56**, 1941 (1995).

[6] T. Jacobs, S. Sridhar, Q. Li, G. D. Gu, and N. Koshizuka, *Phys. Rev. Lett.* **75**, 4516 (1995).

[7] T. Shibauchi, N. Katase, T. Tamegai, and K. Uchinokura, *Physica C* **264**, 227 (1996).

[8] H. Srikanth, Z. Zhai, S. Sridhar, and A. Erb, *J. Phys. Chem. Solids* **59**, 2105 (1998).

[9] H. Kitano, T. Hanaguri, and A. Maeda, *Phys. Rev. B* **57**, 10946 (1998).

[10] A. Hosseini, S. Kamal, D.A. Bonn, R. Liang, and W. N. Hardy, *Phys. Rev. Lett.* **81**, 1298 (1998).

[11] A. Buzdin and D. Feinberg, *Phys. Lett.* **A165**, 281 (1992).

[12] N. E. Hussey, A. Carrington, J. R. Cooper, and D. C. Sinclair, *Phys. Rev. B* **50**, 13073 (1994).

[13] L. N. Bulaevskii, V. L. Pokrovsky, and M. P. Maley, *Phys. Rev. Lett.* **76**, 1719 (1996).

[14] A. E. Koshelev, *Phys. Rev. Lett.* **76**, 1340 (1996).

[15] Y. Matsuda, M. Gaifullin, K. Kumagai, M. Kosugi, and K. Hirata, *Phys. Rev. Lett.* **8**, 1972 (1997).

[16] E. Sonin, *Phys. Rev. Lett.* **79**, 3732 (1997).

[17] C. E. Gough and N. J. Exon, *Phys. Rev. B* **50**, 488 (1994).

[18] D. V. Shovkun, M. R. Trunin, A. A. Zhukov, Yu. A. Nefyodov, H. Enriquez, N. Bontemps, A. Buzdin, M. Daumens, and T. Tamegai, *JETP. Lett.* **71**, 92, 2000.

[19] We note that $\delta f(T)$ includes the frequency shift due to the sample thermal expansion, which is essential for $T > 0.7\,T_c$ in the T-orientation[1].

[20] M. R. Trunin, Yu. A. Nefyodov, and H. J. Fink, cond-mat/9911211 (submitted to JETP).

[21] H. Enriquez, N. Bontemps, A.A. Zhukov, D.V. Shovkun, M.R. Trunin, A. Buzdin, M. Daumens, and T. Tamegai, submitted.

[22] N. Bontemps, H. Enriquez, and Y. DeWilde, *Physics and Materials Science of Vortex states, Flux Pinning and Dynamics*, NATO Science Series 356 Ed. R. Kossovsky, S. Bose, W. Pan, and Z. Durusoy 387 (1999).

[23] J. R. Clem, M. W. Coffey, and Z. Hao, *Phys. Rev. B* **44**, 2732 (1991).

[24] A. Schilling, F. Hulliger, and H. T. Ott, *Z. Phys. B* **82**, 9 (1991).

[25] S-F. Lee, D. C. Morgan, R. J. Ormeno, D. M. Broun, R. A. Doyle, and J. R. Waldram, *Phys. Rev. Lett.* **77**, 735

(1996).

[26] T. Tamegai, M. Sato, A. Mashio, T. Shibauchi, and S. Ooi, *Proceedings of the 9th International Symposium on Superconductivity*, Advances in Superconductivity IX, Ed. S. Nakajima and M. Murakami, 621, Springer-Verlag Tokyo (1997).

[27] N. Nakamura, G. D. Gu, and N. Koshizuka, *Phys. Rev. Lett.* **71**, 915 (1993).

[28] F. Steinmeyer, R. Kleiner, P. Müller, H. Müller, and K. Winzer, *Europhys. Lett.* **25**, 459 (1994).

[29] O.K.C. Tsui, N. P. Ong, and J. B. Peterson, *Phys. Rev. Lett.* **76**, 819 (1996).

[30] B. Khaykovich, E. Zeldov, D. Majer, T. W. Li, P. Kes, and M. Konczykowski, *Phys. Rev. Lett.* **76**, 2555 (1996).

[31] C. P. Bean and J. B. Livingston, *Phys. Rev. Lett.* **12**, 14 (1964).

[32] P. G. De Gennes, *Superconductivity of Metals and Alloys*, Benjamin, NY, (1996).

8